

Alfvénic Turbulence Beyond the Ambipolar Diffusion Scale

Blakesley Burkhart^{1,2}, A. Lazarian², D. Balsara³, C. Meyer³, J. Cho⁴

¹ *Harvard-Smithsonian Center for Astrophysics, 60 Garden St., Cambridge, MA 0213*

² *Astronomy Department, University of Wisconsin, Madison, 475 N. Charter St., WI 53711, USA*

³ *Department of Physics, University of Notre Dame, Notre Dame, IN 46556, USA*

⁴ *Department of Astronomy and Space Science, Chungnam National University, Daejeon, Korea*

ABSTRACT

We investigate the nature of the Alfvénic turbulence cascade in two fluid MHD simulations in order to determine if turbulence is damped once the ion and neutral species become decoupled at a critical scale called the ambipolar diffusion scale (L_{AD}). Using mode decomposition to separate the three classical MHD modes, we study the second order structure functions of the Alfvén mode velocity field of both neutrals and ions in the reference frame of the local magnetic field. On scales greater than L_{AD} we confirm that two fluid turbulence strongly resembles single fluid MHD turbulence. Our simulations show that the behavior of two fluid turbulence becomes more complex on scales less than L_{AD} . We find that Alfvénic turbulence can exist past L_{AD} when the turbulence is globally super-Alfvénic, with the ions and neutrals forming separate cascades once decoupling has taken place. When turbulence is globally sub-Alfvénic and hence strongly anisotropic with a large separation between the parallel and perpendicular decoupling scales, turbulence is damped at L_{AD} . We also find that the power spectrum of the kinetic energy in the damped regime is consistent with a k^{-4} scaling (in agreement with the predictions of Lazarian, Vishniac & Cho 2004).

Subject headings: turbulence, waves, magnetohydrodynamics (MHD)

1. Introduction

Turbulence and magnetic fields are critical components of the interstellar medium (ISM) of galaxies from kiloparsec to sub-astronomical unit scales. Magnetohydrodynamic (MHD)

turbulence is a key element in the study of star formation and molecular cloud structure, magnetic reconnection, heat transport and cosmic ray propagation (see Elmegreen & Scalo 2004; Ballesteros-Paredes et al. 2007; Mckee & Ostriker 2007; Tilley & Balsara 2006; Tilley, Balsara, & Howk 2006; Balsara et al. 2008; Brandenburg & Lazarian 2013). Despite the importance of turbulence for ISM studies, many mysteries remain, including the nature of turbulence driving and damping scales.

The smallest scales of the turbulence cascade, including the damping scale, may play a pivotal role in the dynamics of giant molecular clouds (GMCs) and star formation. GMCs are partially ionized, with neutrals coupled to the magnetic field through collisions with ions. The drift of the neutrals towards the central gravitational potential through the ionized particles tied to the magnetic field, known as ambipolar diffusion, is an often invoked source of dissipation of the MHD cascade (Zweibel & Josafatsoon 1983; Ciolek & Basu 2000; Tassis & Maouschovias 2004). The ambipolar diffusion scale (L_{AD}), or the scale at which neutrals and ions decouple, has been thought to set the dissipation scale of turbulence in molecular clouds and to set a fundamental characteristic scale for gravitational collapse and star formation (Balsara 1996; Houde et al. 2000; Klessen, Heitsch & Mac Low 2000; Li et al. 2006; Li & Houde 2008; Li et al. 2008; Hezareh et al. 2010; Tilley & Balsara 2010; Meyer et al. 2014).

The ambipolar diffusion scale can be estimated as the scale at which the Reynolds number, with diffusivity given by the ambipolar diffusivity, is equal to unity (Brandenburg & Zweibel 1994, 1995; Balsara 1996; Oishi & Mac Low 2006). The ambipolar diffusivity is given by

$$\nu_{AD} = \frac{B^2}{4\pi\rho_i\rho_n\alpha} \quad (1)$$

where ρ_i and ρ_n are the density of the ions and neutrals, B is the magnetic field strength, and α is the frictional coupling coefficient¹ between the ions and neutrals.

The Reynolds number for ion-neutral drift is defined as:

$$R_{AD} = \frac{LV}{\nu_{AD}} \quad (2)$$

where V is a characteristic velocity (e.g. for trans-Alfvénic turbulence it is the Alfvén speed, $V_A = \frac{B}{\sqrt{4\pi\rho_n}}$) and $L=L_{AD}$ when $R_{AD}=1$. This gives the form of the ambipolar diffusion scale as often found in the literature:

$$L_{AD} = V_A/\alpha\rho_i \quad (3)$$

¹ α is often denoted as γ in the literature. However, in this work we use the notation α as it was used in Meyer et al. 2014 for consistency with this previous work.

More details about the derivation and significance of L_{AD} can be found in a number of works including Langer (1978); Zweibel & Josafattsson (1982), Balsara (1996), Klessen Heitsch & Mac Low (2000), Oishi & MacLow (2006), Li & Houde (2008), Hezareh et al. (2010) and Meyer et al. (2014)

The application of ambipolar diffusion extends beyond direct studies of star formation to include general studies of magnetic fields. For example, Houde et al. (2000); Li & Houde (2008), and Hezareh et al. (2010) have proposed that the magnetic field in the plane of the sky may be obtained from observations via calculation of the ambipolar diffusion length scale. In light of these diverse interpretations of the meaning of L_{AD} it is important to understand to what extent L_{AD} is relevant to turbulence damping in partially ionized gasses.

More generally, ambipolar diffusion has also been proposed to damp particular families of linear MHD waves (see Balsara 1996 and ref. therein). On scales larger than L_{AD} it was predicted that two fluid turbulence acts like single fluid MHD turbulence. In particular, Balsara (1996) on the basis of 1D dispersion analysis, showed that two separate mode damping situations can occur at scales at or smaller than L_{AD} , which are based on the value of plasma beta (i.e. the ratio of the gas to magnetic pressure). When the Alfvén speed is greater than the sound speed, the fast and Alfvén wave families are damped at or below L_{AD} . When the Alfvén speed is smaller than the sound speed, the slow and Alfvén wave families are damped. For either high or low plasma beta, Balsara (1996) predicts that the Alfvénic waves should damp at L_{AD} and thus the MHD cascade should damp past the ambipolar diffusion scale. To put Balsara (1996) in context, large scale 3D MHD simulations were not possible at the time. Tilley & Balsara (2011) have extended the study of Balsara (1996) to include flows with radiative effects. They find that the general analysis of the MHD wave modes that are damped remained unchanged.

Does MHD turbulence, specifically the Alfvén modes, damp at the decoupling scale L_{AD} ? MHD turbulence is known to be different from a collection of linear Alfvénic waves. Cascading rates and the anisotropy of turbulence should be accounted for carefully before we can make a definitive conclusion about turbulent damping in the partially ionized media. The purpose of this paper is to address the question above numerically, as well as to numerically test the validity the Alfvén mode scaling relations of the Goldreich & Sridhar (1995, henceforth GS95) theory for ion-neutral turbulence. The GS95 theory was first extended to a partially ionized compressible medium in subsequent works by Lithwick & Goldreich (2001, henceforth LG01) and Lazarian et al. (2004, henceforth LVC04). In this paper we will apply the Cho & Lazarian (2002, 2003; henceforth CL02, CL03, respectively) MHD mode decom-

position technique² to two-fluid MHD simulations, first presented in Meyer et al. (2014), in order to investigate the behavior of the Alfvén modes in the ions and neutrals. Our paper is organized as follows: in Section 2 we review the basic scaling relations predicted by the GS95 model, in Section 3 we describe the numerical simulations and relevant scales, in Section 4 we present the structure function scalings for the the full data cubes and the Alfvénic modes of the ions and neutrals for our simulations and finally in Section 5 we discuss our results followed by our conclusions in Section 6.

2. The GS95 scalings

MHD turbulence is a subject with an extended history (see book by Biskamp 2003). However, it has been given a boost more recently with the advent of 3D MHD simulations which have allowed for testing theoretical predictions (see recent reviews by Brandenburg & Lazarian 2013; Beresnyak & Lazarian 2014). The modern theory of MHD turbulence is based on the Goldreich-Sridhar (1995, GS95) idea which was extended and tested in subsequent publications (Lazarian & Vishniac 1999, Cho & Vishniac 2000, Maron & Goldreich 2001, Cho & Lazarian 2002, 2003, henceforth CL02, CL03, respectively). The applicability of GS95 theory to the partially ionized gas was discussed in Lithwick & Goldreich (2001) and Lazarian et al. (2004).

It has been shown numerically, that in the presence of dynamically important magnetic fields eddies become elongated along the magnetic field lines. GS95 approach to Alfvénic modes can be easily understood: For the eddies perpendicular to the magnetic field, the original Kolmogorov energy scaling applies, i.e. $V_l \sim l_\perp^{1/3}$, where l_\perp denotes scales measured perpendicular to the local magnetic field. Mixing motions induce Alfvénic perturbations that determine the parallel size of the magnetized eddy. This is the concept of *critical balance* i.e. the equality of the eddy turnover time (l_\perp/V_l) and the period of the corresponding Alfvén wave $\sim l_\parallel/V_A$, where l_\parallel is the parallel eddy scale and V_A is the Alfvén velocity. Making use of $V_l \sim l_\perp^{1/3}$, one finds the scaling relation for the parallel and perpendicular eddies as: $l_\parallel \sim l_\perp^{2/3}$. This represents the scale dependent tendency of eddies to become more elongated along the magnetic field lines as the energy cascades proceeds to smaller scales and corresponds to the scaling of the slow and Alfvén wave anisotropy. The power spectrum for the slow and Alfvén waves scales as $E \sim k_\perp^{-5/3}$ (see review by Brandenburg & Lazarian 2013). Numerical studies of scaling of compressible MHD turbulence based on the decomposition into Alfvén,

²A different decomposition technique based on wavelet analysis is used in Kowal & Lazarian 2010, but the results of the two different procedures of decomposition are similar.

Slow and Fast modes were first performed in CL02 and CL03 and these results were later reconfirmed in Kowal & Lazarian (2010) with a wavelet approach.

GS95 theory assumes the isotropic injection of energy at scale L and the injection velocity equal to the Alfvén velocity in the fluid V_A , i.e. the Alfvén Mach number $M_A \equiv (V_L/V_A) = 1$. The GS95 model was later generalized for both sub-Alfvénic, i.e. $M_A < 1$, and super-Alfvénic, i.e. $M_A > 1$, cases (see Lazarian & Vishniac 1999 and Lazarian 2006) and thus the simulations used in this paper (which are sub- and super-Alfvénic) should be understood in this context. In the next two paragraphs we provide a brief synopsis of the differences of single fluid turbulence with $M_A > 1$ and $M_A < 1$.

For $M_A > 1$ magnetic fields are not dynamically important at the largest scales and hence turbulence from the driving scale (L) to a transition scale L_A follows an isotropic cascade. At scales smaller than L_A , critical balance occurs and scale dependent anisotropy proceeds down to the dissipation range. Scale L_A is given by:

$$L_A = L(V_A/V_L)^3 = LM_A^{-3} \quad (4)$$

and the relationship between parallel and perpendicular scales that occurs at scales smaller than L_A is:

$$l_{\parallel} \sim L(l_{\perp}/L)^{2/3}M_A^{-1}, \quad M_A > 1, \quad (5)$$

where \parallel and \perp are relative to the direction of the local magnetic field.

Similarly, for $M_A < 1$, turbulence does not obey the GS95 scaling starting at scale L , but from a smaller scale L_{trans} , as it transitions from weak to strong turbulence:

$$L_{trans} \sim L(V_L/V_A)^2 \equiv LM_A^2 \quad (6)$$

In the range $[L, L_{trans}]$ the turbulence is “weak,” meaning that it is dominated by interacting MHD waves, rather than eddies.

For scales less than L_{trans} the turbulence is eddy-like (i.e. strong) and it follows a GS95-type scalings:

$$l_{\parallel} \sim L(l_{\perp}/L)^{2/3}M_A^{-4/3}, \quad M_A < 1. \quad (7)$$

CL02, CL03 and Kowal & Lazarian (2010) focused their analysis and comparisons with theoretical predictions of single fluid MHD turbulence simulations. Ions and neutrals are generally expected to behave as a single MHD fluid at length scales from L_{trans} or L_A to scale $L_{AD} = V_A/\alpha\rho_i$. At scales smaller than L_{AD} , the ion and neutral energetics separate and MHD turbulence may dissipate (Zweibel & Josafatsoon 1983; Balara 1996; Klessen 2000).

All these above mentioned studies assumed that the diffusivities arising from viscosity and resistivity are the same, i.e. that the Prandtl number of turbulence is unity³. However, viscosity induced by neutrals can result in a very different regime of turbulence. The high Prandtl number MHD turbulence was described theoretically in Lazarian et al. (2004, henceforth LVC04) with numerical simulations published in Cho, Lazarian & Vishniac (2002, 2003). In this regime, magnetic and kinetic energy spectra are different with theoretical predictions for the kinetic energy $E_K \sim k^{-4}$ and magnetic energy $E_M \sim k^{-1}$ (LVC04). These predictions agree with single fluid MHD numerical simulations and we therefore use these studies as a touchstone for our analysis. At the same time, it would be an oversimplification to assume that turbulence in a partially ionized gas is equivalent to high Prandtl number turbulence. It can have some features of it, but ion-neutral damping of turbulent motions as well as the decoupling of ion and neutrals change the picture in a significant way (Lithwick & Goldreich 2002, LVC04, Xu et al. 2014, Lazarian & Yan 2014). Therefore in what follows we investigate numerically how MHD turbulence evolves in the partially ionized gas.

3. Numerical Scheme and Mode Decomposition

We use the simulations first presented in Meyer et al. 2014 and reference to that work for the details of the numerical setup and provide here only the essential points for this work.

The MHD capabilities of the RIEMANN code (Balsara 1998a,b; Balsara & Spicer 1999a,b; Balsara 2004, 2010, 2012) have recently been upgraded to treat two-fluid MHD. In two-fluid MHD, the ambipolar effects are modeled with a neutral fluid obeying the isothermal Euler equations and an ionized fluid which obeys the isothermal MHD equations (Tilley & Balsara 2008; Tilley, Balsara & Meyer 2011). The two-fluid version of RIEMANN has been applied to astrophysical turbulence in our prior papers (Tilley & Balsara 2010, Meyer et al. 2014). A variety of higher order reconstruction methods are available in our code and we used r=3 WENO reconstruction (Jiang & Shu 1996, Balsara & Shu 2000) because it represents a good compromise between accuracy and speed. The density of the neutrals was scaled to unity and the mean molecular weights of the neutrals and ions were given by $\mu_N = 2.3$ amu and $\mu_i = 29$ amu (corresponding to HCO+) respectively. Consequently, for a particular ionization fraction χ , the ion density is given by $\rho_i = \chi \rho_N \mu_i / \mu_N$. The magnetic field was initialized along the x-direction. The simulations were started with uniform density

³The Prandtl number mentioned here is defined as $\text{Pr} = \nu / \eta$, where η is magnetic resistivity and ν is fluid viscosity. Here we make the notational extension that $\text{Pr}_{AD} = \nu_{AD} / \eta$. Since the fluid diffusivity (ν) is much smaller than ν_{AD} we expect $\text{Pr} > 1$.

in the ions and neutrals, and they were forced via random Gaussian fluctuations (peaked at $k = 2$ and spanning $1 \leq k \leq 4$) into a turbulent state so that the desired Mach numbers were represented in the velocity field. Once a steady state was reached, the simulations were continued for a few further turn over times so that statistics of the two-fluid turbulence could be gathered.

In this paper, we investigate three forced turbulence simulations at resolution 512^3 . We set the Alfvén speed for the combined fluid to be 1, 3 and 6 times the sound speed. We refer to these runs as A1, A3 and A6 respectively. Three obvious scales of interest exist in these simulations: the turbulence driving scale (L), the ambipolar diffusion scale (L_{AD}) and the numerical dissipation scale, which begins around 10-20 grid units. We note that in the regime of strong MHD turbulence, one must think of the ambipolar diffusion scale in both the direction parallel and perpendicular to the mean magnetic field, i.e. $L_{AD\parallel}$ and $L_{AD\perp}$, respectively. $L_{AD\parallel}$ as set in the code is given by $L_{AD\parallel} = v_A/\alpha\rho_i$. $L_{AD\perp}$ is given by either Equation 5 or 7 depending on if the turbulence is super-Alfvénic or sub-Alfvénic, respectively. We list values of $L_{AD\perp}$ in Table 1 for the range of driving scales, i.e. from $L=512-128$. Table 1 also provides the values for L , $L_{AD\parallel}$, as well as the transition between weak and strong turbulence (l_{trans}) for models A3 and A6 as given by equation 2 and, for the super-Alfvénic model A1, the transition scale between hydrodynamic and MHD turbulence (L_A) given by equation 4. In columns two, three and four of Table 1 we list the sonic Mach number and the volume averaged neutral-ion Alfvén Mach number.

We perform mode decomposition of the velocity field of the ions and neutrals as described in Cho & Lazarian (2003). We briefly summarize this procedure and direct the reader to the original work by Cho & Lazarian (2003) for a more detailed presentation. The slow and fast velocity components can be obtained by projecting the velocity Fourier component v_k onto ξ_s and ξ_f , where ξ_f and ξ_s are the basis vectors for the slow and fast modes, respectively, which lie in the plane defined by the mean magnetic field direction \mathbf{B}_0 and \mathbf{k} . They are defined as:

$$\hat{\xi}_s \propto (-1 + \alpha_a - \sqrt{D})k_{\parallel}\hat{\mathbf{k}}_{\parallel} + (\mathbf{1} + \alpha - \sqrt{D})\mathbf{k}_{\perp}\hat{\mathbf{k}}_{\perp} \quad (8)$$

Table 1: Description of the simulation parameters

Run	M_s	$\langle M_A \rangle$	χ	$L_{AD\perp}$	$L_{AD\parallel}$	L_A	l_{trans}	L_{Drive}
A1	3.0	1.8	10^{-4}	58-9	40	77	N/A	512-128
A3	2.5	0.7	10^{-4}	33-16.4	80	N/A	256	512-128
A6	2.5	0.4	2×10^{-4}	11-5.3	80	N/A	86	512-128

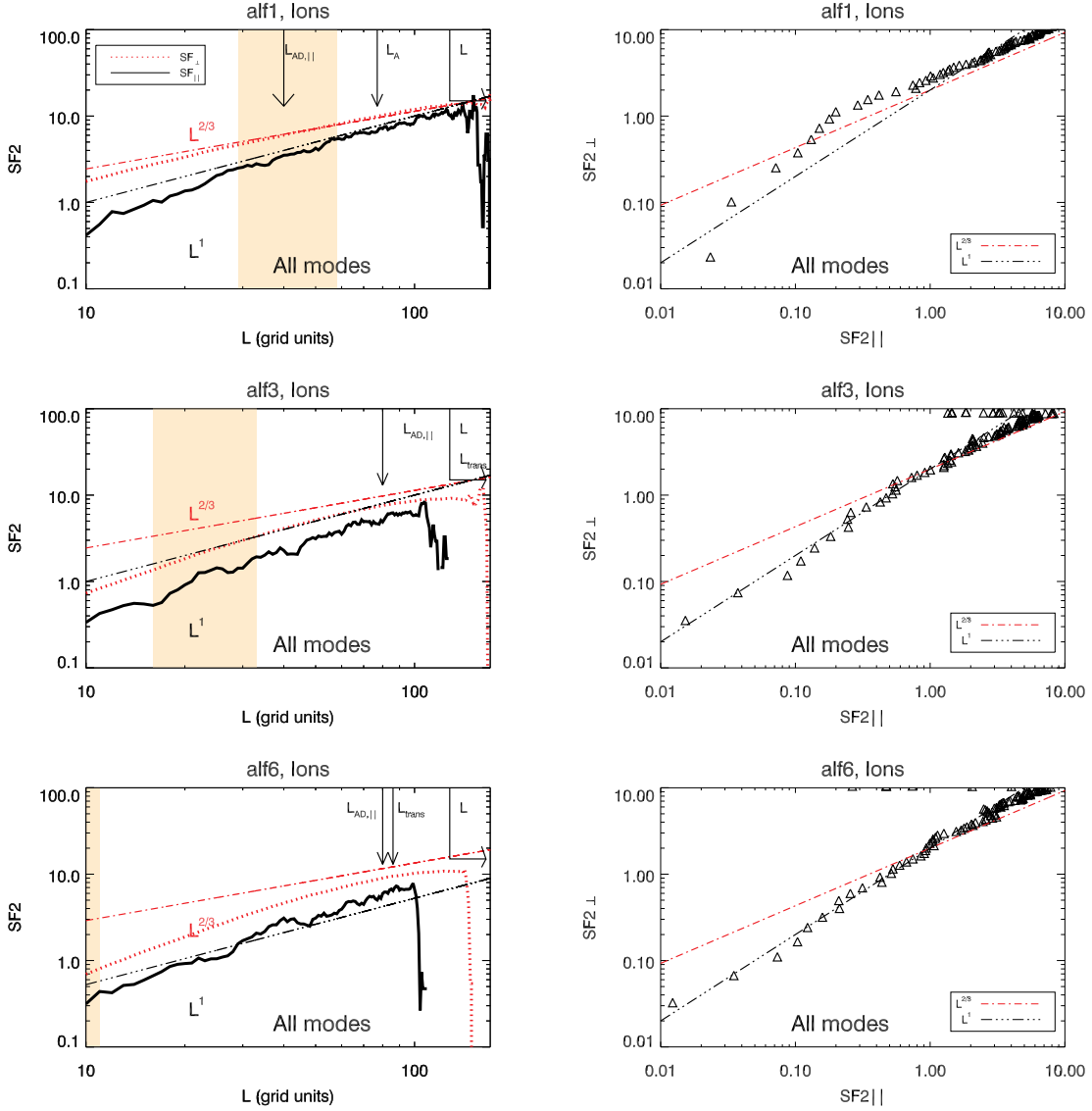


Fig. 1.— Structure functions of the ion velocity field in the local frame of reference. The two columns both show the structure function and their predicted scalings (red color lines for the perpendicular and black color lines for the parallel scaling). The first column shows both parallel and perpendicular structure functions vs. scale while the second column plots the parallel vs. perpendicular structure functions. Row one present the results for model A1 (which is super-Alfvénic) and row two and three present results for models A3 and A6 (sub-Alfvénic), respectively. In the left column, we indicate the presence of several important scales: the driving scale (L), the parallel ambipolar diffusion scale ($L_{AD,\parallel}$), the perpendicular ambipolar diffusion scale (range of tan box using driving scales from 512-128 pixels), and the transition scale to GS95 (L_A for model A1 and L_{trans} for models A3 and A6).

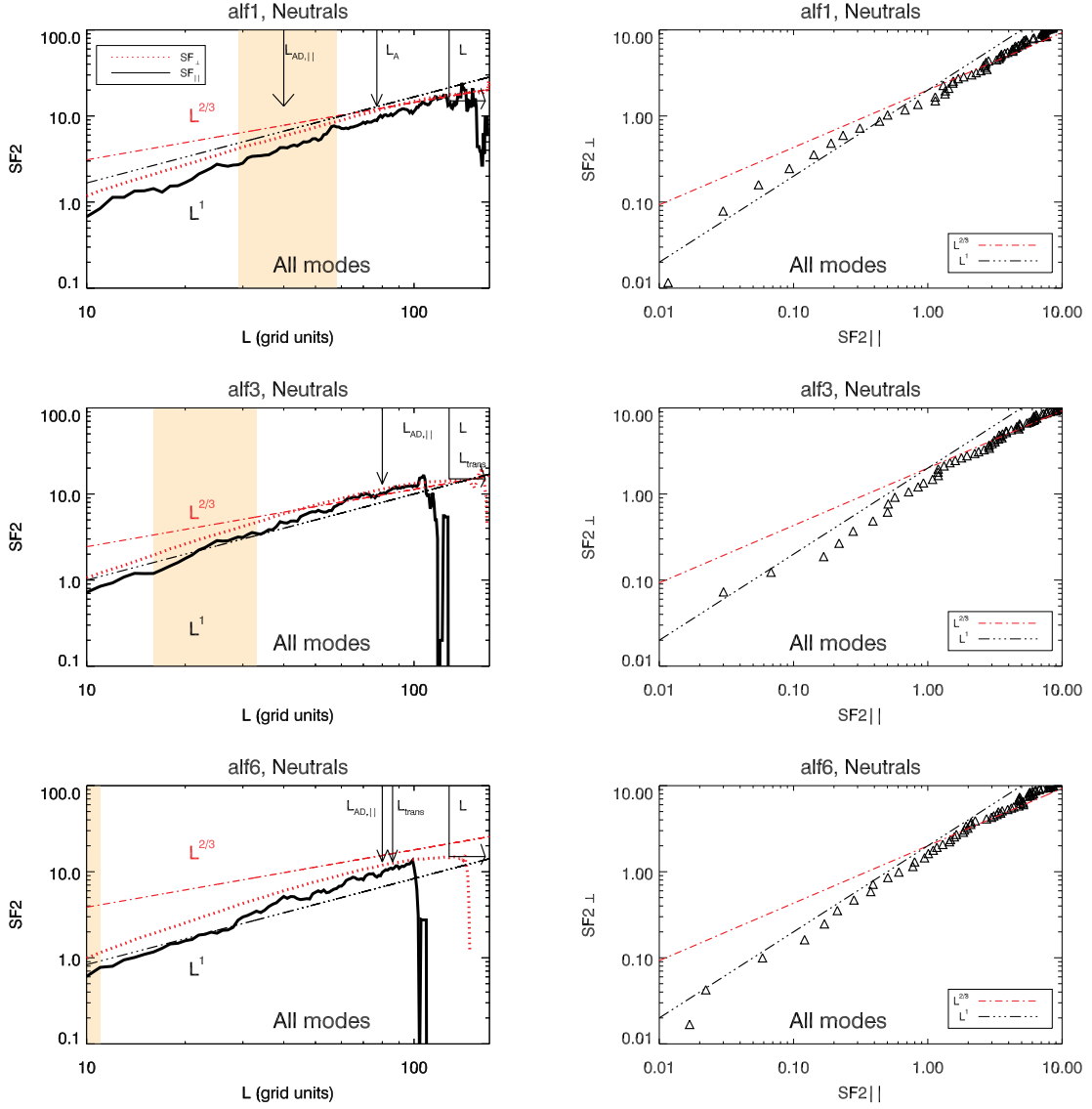


Fig. 2.— Structure functions of the neutral velocity field in the local frame of reference. The figure is organized in an identical manner to Figure 1).

$$\hat{\xi}_f \propto (-1 + \alpha_a + \sqrt{D})k_{\parallel}\hat{\mathbf{k}}_{\parallel} + (\mathbf{1} + \alpha + \sqrt{D})\mathbf{k}_{\perp}\hat{\mathbf{k}}_{\perp} \quad (9)$$

and the basis vector for the Alfvén mode is:

$$\hat{\xi}_A = \mathbf{k}_{\perp} \times \hat{\mathbf{k}}_{\parallel} \quad (10)$$

where $D = (1 + \alpha_a)^2 - 4\alpha_a \cos(\theta)$, $\alpha_a = c_s^2/V_A^2 = \beta(\gamma/2)$. θ is the angle between \mathbf{k} and \mathbf{B}_0 , c_s is the sound speed and γ is the adiabatic index. These expressions for the mode decomposition basis are rigorously derived in Appendix A of Cho & Lazarian (2003) and illustrated in their Figure 2.

4. Results

4.1. Velocity scaling without mode decomposition

First we investigate the structure functions of the velocity field in the local frame relative to the mean magnetic field. In this subsection we present our results *without* mode decomposition. We calculate the structure functions:

$$SF_2(\mathbf{r}) = \langle |\mathbf{v}(\mathbf{x} + \mathbf{r}) - \mathbf{v}(\mathbf{x})|^2 \rangle \quad (11)$$

in which we obtain separately the cases in which the axis is aligned parallel and perpendicular with the *local* mean field

We present the structure function analysis for the ion velocity field in Figure 1 and for the neutral velocity field in Figure 2. In the ions for all simulations, the GS95 scaling is observed till $L_{AD,\parallel}$ and there is a range of scales in which the scaling of $l^{2/3}$ can be seen for all models in the right column panels. Model A1 (top panels) is super-Alfvénic and thus the transition to strong turbulence and the GS95 scaling does not begin until scale $L_A \approx 77$ grid units however past this scale a scaling of $l^{2/3}$ is clearly seen down to $L_{AD,\parallel}$

Models A3 and A6 (middle and bottom panels, respectively), are sub-Alfvénic and thus are in the regime of weak or wave-like turbulence until scale L_{trans} given in Table 1. Both A3 and A6 have $L_{AD,\parallel}$ and $L_{AD,\perp}$ separated by a larger dynamic range of scales than model A1 due to sub-Alfvénic turbulence. At scales smaller than the driving scale and L_{trans} , Alfvénic turbulence in the ions develops and is clearly seen in the left column panels by the scaling relation $l_{\parallel} \sim l^{2/3}$. For models A3 and A6, the range of scales for GS95 is limited (as seen in the right column panels), as either the driving scale or L_{trans} is close to $L_{AD,\parallel}$. However for

model A1 the range of L_{AD} is separated from both L and L_A with sufficient dynamic range to generate an Alfvénic cascade with the GS95 scaling in the ions.

The neutral structure functions shown in Figure 2 also have GS95 scalings until $L_{AD,\parallel}$ in all three simulations studied. At $L = L_{AD,\parallel}$ neutrals decouple from the ions and no longer exhibit the scaling relations of an MHD cascade. The $l^{2/3}$ scaling is present in the neutrals until $L=40$ for model A1. Model A3 and A6 transition to an l^1 scaling at larger scales than model A1 with model A6 transitioning to l^1 at slightly larger scales than model A3. Since models A3 and A6 have identical values for $L_{AD,\parallel}$ this suggests that the driving scale and/or Alfvén Mach number also plays a role in the dissipation scale of partially ionized fluid turbulence. It is also interesting to note that in the A1 model the ions exhibit a greater dynamic range than the neutrals over which the $l^{2/3}$ is observed. This suggests that the ions may continue the MHD cascade even after they have decoupled from the neutrals. As most of the energy in the MHD cascade lies in the Alfvén modes (see Kowal & Lazarian 2010) it is important to determine if the damping of the cascade at these scales is due to damping in the Alfvén modes.

4.2. Velocity scaling with mode decomposition

In order to address the nature of the Alfvénic cascade in ion-neutral turbulence we must separate the Alfvén modes from the Fast and Slow modes. We perform the mode decomposition on the the ion and neutral velocity fields to extract the Alfvén modes and then apply the second order structure function analysis as was shown in Figures 1 and 2.

We show the ion Alfvén mode structure functions in Figure 3. The Alfvén modes of model A1 (top left panel) obey the GS95 scalings to scales smaller than the ambipolar diffusion scale which indicates that the Alfvénic cascade can continue to scales smaller than L_{AD} . This suggests that turbulence does not necessarily damp at the ambipolar diffusion scale but can continue to the viscous dissipation scale and would not necessarily provide a characteristic scale for star formation, in agreement with Oishi & Mac Low (2006).

Unlike model A1, Alfvénic turbulence in the ions begins to damp at larger scales for model A3 and A6. Alfvénic turbulence in models A3 and A6 damps at or before the perpendicular ambipolar diffusion scale. The larger dynamic range of scales between $L_{AD,\parallel}$ and $L_{AD,\perp}$ coupled with the limited dynamic range between the driving scale and $L_{AD,\parallel}$, increases the effect of damping due to ion-neutral collision. In addition, the strength of the damping due to ion-neutral collisions goes as V_A^2 (Klessen et al. 2000) and explains why the damping is the strongest for model A6.

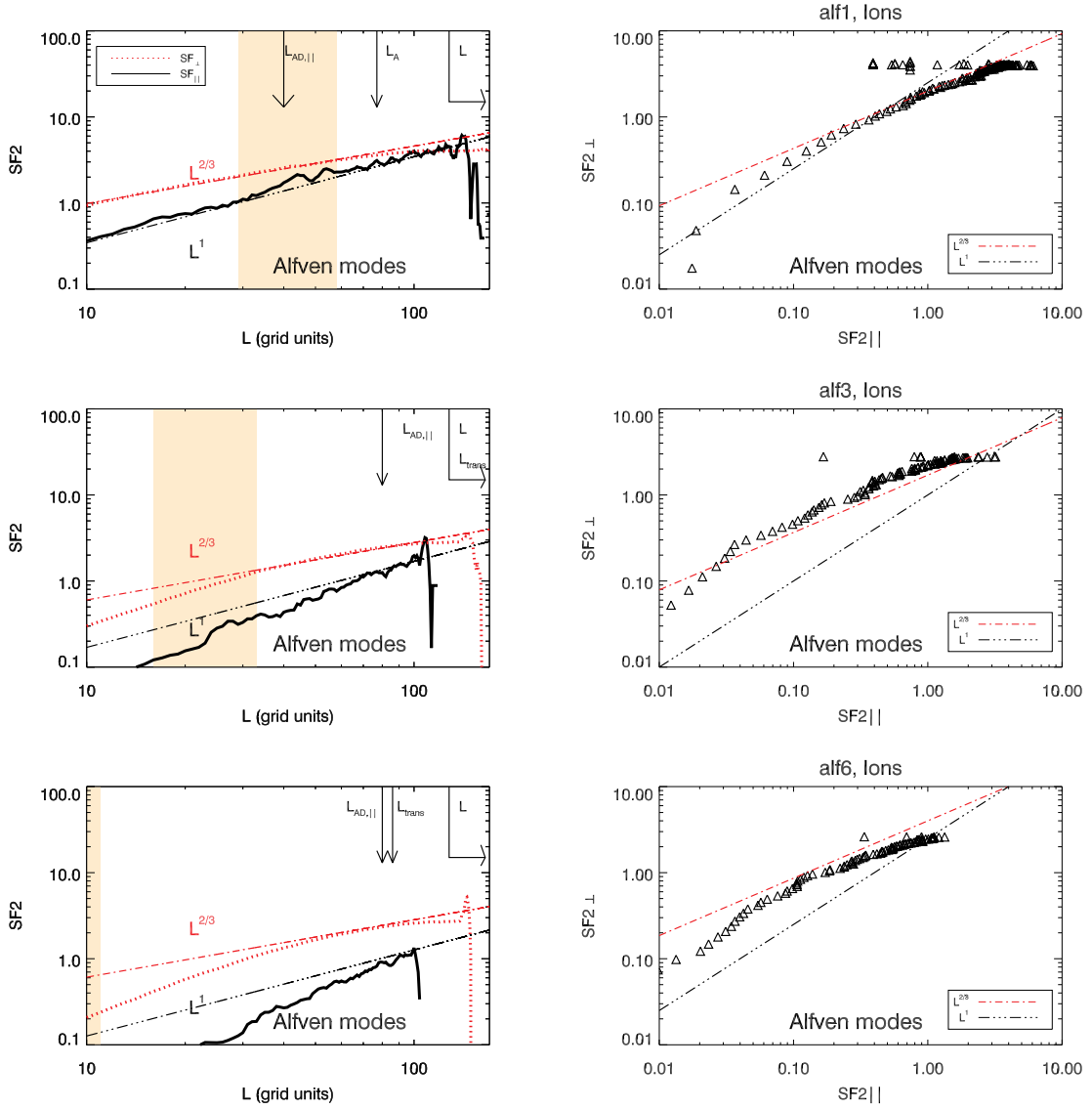


Fig. 3.— Structure functions for the Alfvén modes of the ion velocity field. The figure is organized in an identical manner to Figure 1.

Figure 4 plots the structure functions of the Alfvén mode neutral velocity field of each model in Table 1. The organization of the figure is identical to Figure 3.

In all simulations, the Alfvén mode scaling in the neutrals are seen at large scales but break off from the GS95 scaling at scales smaller than $L_{AD,\parallel}$ and/or $L_{AD,\perp}$. In all three models the perpendicular motions do not follow $l_{\parallel} \sim l^{2/3}$ at scales smaller than $L_{AD,\parallel}$ but another effect seen is that both l_{\parallel} and l_{\perp} begin to steepen to slopes greater than l^1 . This is close to the numerical dissipation scale but also most-likely an unphysical effect due to the fact that once the neutrals decouple from the ions we can no longer apply mode decomposition as Alfvén modes will not exist in the neutral cascade.

What are the possible damping mechanisms that can explain the behavior seen in these simulations? The role of neutral-ion damping in MHD turbulence has been discussed previously in the context of the ISM (in particular, see Spangler 1991; Minter & Spangler 1997; LG01; LVC04). In a partially ionized medium a combination of neutral particle viscosity and ion-neutral collisional coupling drives damping. Neutral-ion friction will compete with and eventually dominate the Alfvén wave restoring force which will damp oscillations in the magnetic field. As soon as the neutral-ion collisional rate is approximately equal to the eddy turnover time, the neutrals will begin to form a hydrodynamic cascade. At this scale, and all smaller scales, the ionic fluid motions will damp at the rate of ion-neutral collisions. The damping mechanism in A3/A6 is most likely the result of ion-neutral collisions however an additional damping mechanism will be provided by neutral viscosity, which may be non-negligible in dissipating the MHD cascade in partially ionized gases (LVC04).

4.3. Power Spectrum

Finally, we investigate the kinetic energy spectra for simulation with and without mode decomposition. We calculate the energy power spectra as:

$$P(\vec{k}) = \sum_{\vec{k}=const.} \tilde{A}(\vec{k}) \cdot \tilde{A}^*(\vec{k}) \quad (12)$$

In hydrodynamic turbulence the viscous damping scale sets a minimal scale for turbulent motions and the kinetic energy power spectrum is dissipated exponentially. This marks the end of the hydrodynamic cascade, but in MHD turbulence the viscous damping scale is not the end of magnetic structure evolution. On these scales magnetic field structures will be created by shear and magnetic tension. As a result, LVC04 predicted a power-law tail in the energy distribution, rather than an exponential cutoff.

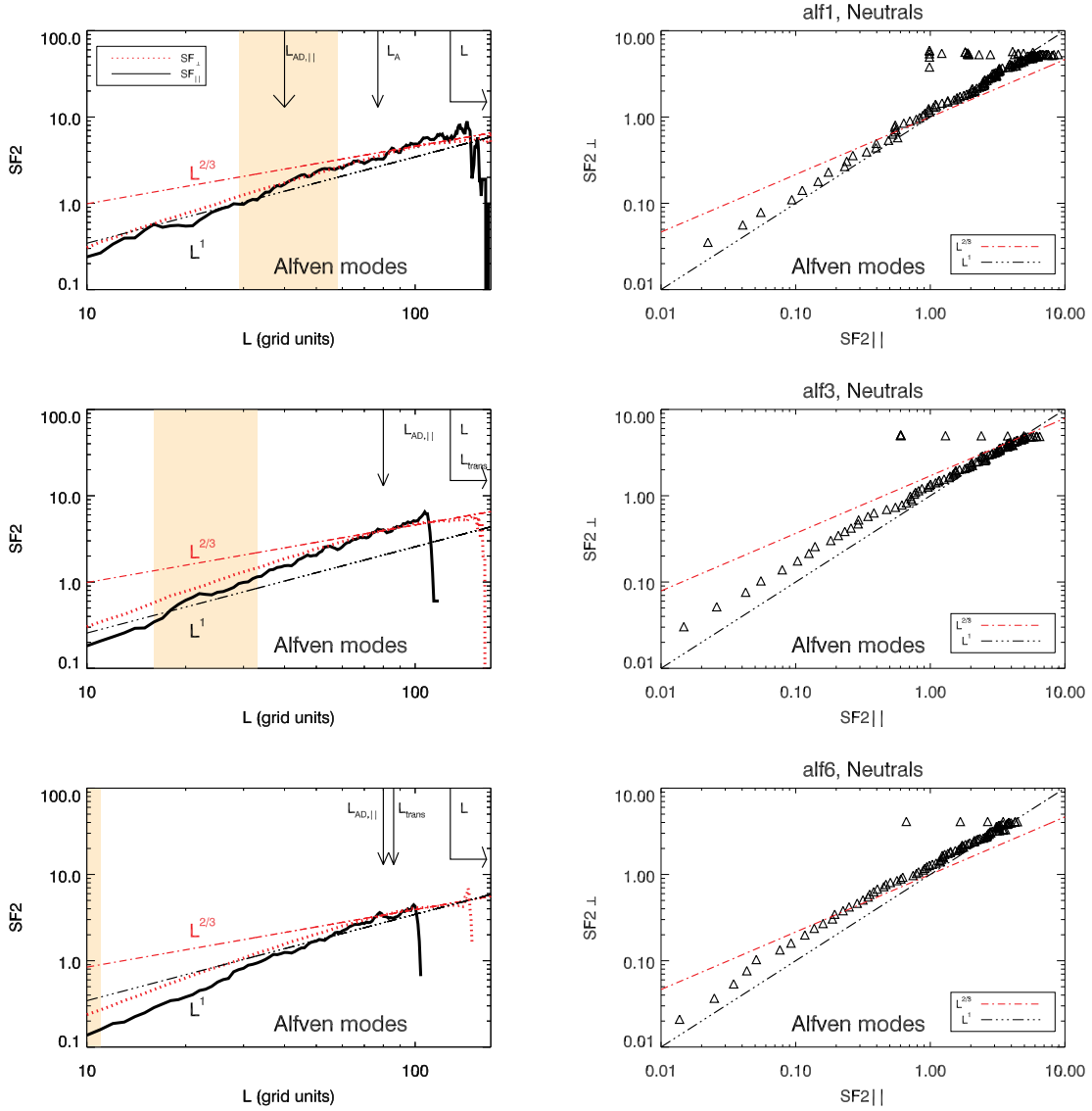


Fig. 4.— Structure functions for the Alfvén modes of the neutral velocity field. The figure is organized in an identical manner to Figure 1. Once the neutrals have decoupled from the ions the mode decomposition to separate the Alfvén modes from the fast and slow modes is no longer a physically motivated procedure.

Figure 5 shows the neutral kinetic energy power spectrum (black lines) and the ion kinetic energy power spectrum (red lines) for models A1, A3 and A6. For model A1, the neutral Alfvén modes damp out well before the ion Alfvén modes. The ions retain the $k^{-5/3}$ even after the neutrals have decoupled. For models A3 and A6, there is a small portion of the spectrum with the $k^{-5/3}$ scaling for the Alfvén mode in the ions which is not noticeable in the neutrals due to the limited dynamic range over which the Alfvén modes propagate. In the high k damped regime, the slopes approaches k^{-4} rather than behaving as an exponential decay of energy. This result should be confirmed with higher resolution simulations in the future.

5. Discussion

Supersonic MHD turbulence is known to play a critical role in both the support of GMCs and their subsequent small scale collapse. Ambipolar diffusion has been thought to be the most important dissipation mechanism for turbulence in GMCs and could set characteristic mass and length scales for star formation. However this study shows that turbulence, in particular the Alfvénic cascade, in a partially ionized media does not necessarily damp at the ambipolar diffusion scale L_{AD} . Other authors, for example Oishi & Mac Low (2006), investigated two fluid simulations and found that L_{AD} did not set a characteristic length scale for mass sizes or dissipation and that turbulence may proceed to smaller scales. Previous studies, however, often used the heavy ion approximation which dramatically changes the mode propagation characteristics of two fluid turbulence. We show in this work that Alfvénic modes can survive to scales much smaller than L_{AD} in some cases. This finding also implies that an important diffusion process called reconnection diffusion, which is mediated by turbulence (see Lazarian & Vishniac 1999; LVC04, Lazarian 2005, Santos-Lima et al. 2009, see Lazarian 2014 for a review) may persist to small scales.

The actual damping mechanisms may include neutral particle viscosity and ion-neutral collisions. A detailed investigation of the dominance of one damping mechanism over another is beyond the scope of this work, however comparisons with Equations 37 and 46 of LG01 suggest that the neutral mean free path for our models A3 and A6 is smaller than A1 and hence damping by neutral collisions may play an important role.

While this work is a theoretical and numerical study, our results have very important direct implications for observations. We have shown that the Alfvén Mach number is a critical parameter for obtaining the damping and scaling characteristics of the turbulence which may play a role in the interpretation of velocity dispersion methods of obtaining the ambipolar diffusion scale (Hezareh et al. 2014). Our results fit well in the context of

interpreting the observational signatures of decoupling found in Tilley & Balsara (2010) and Meyer et al. (2014). Meyer et al. (2014) showed that the PDFs of sub-Alfvénic turbulence (i.e. models A3 and A6) were different in the ions and neutrals when looking at a LOS parallel to B, but similar with a sight-line perpendicular to B. As we have shown, the perpendicular decoupling scale for these models occurs at much smaller scales along the cascade, hence density fluctuations maybe coupled in this direction even after the cascade has begun to damp. Contrary to the sub-Alfvénic behavior, Meyer et al. 2014 showed that the PDFs of ions and neutrals for model A1 are very similar and are generally LOS independent, which is expected from our results as turbulence persists in this model to scales smaller than the decoupling scale.

One of our most important findings suggest that the MHD turbulence cascade does not simply damp at the decoupling scale L_{AD} but rather depends on other parameters such as the Alfvén Mach number, which determines the level of anisotropy in the cascade. Furthermore, we show that neutrals and ions behave as a single MHD fluid at certain scales, which can explain the correlation of 21-cm filaments with the magnetic field (Clark, Peek, & Putman 2014). There are several methods to obtain the Alfvén Mach number that extend beyond direct observational techniques such as Zeeman spitting (Crutcher et al. 2009). These include anisotropy in the structure function of velocity centroids (Esquivel & Lazarian 2005; Esquivel & Lazarian 2011; Burkhart et al. 2014), Principle Component Analysis (Correia et al. 2014) and the bispectrum (Burkhart et al. 2009). The power spectrum of partially ionized fluids can also be an indication of the Alfvénic state of the gas, as suggested by Hezareh et al. (2010) and Meyer et al. (2014) and shown in our Figure 5.

Our work shows that the use of scale L_{AD} as the scale for the suppression of the MHD cascade in partially ionized gasses may not be the final story. It is clear that a more detailed theoretical study of turbulence dissipation in partially ionized gas is required in order to understand the precise damping mechanism for a given parameter space (see more in Xu et al. 2014, in prep.)

6. Conclusions

We studied the structure function scaling relations and power spectra of the velocity field Alfvén modes of two fluid (ion-neutral) MHD turbulence. We investigated at what scales MHD turbulence is damped in the partially ionized gas, treating ions and neutral separately. We showed that the GS95 scalings and anisotropy are present in the velocity structure functions of the ions and neutrals in all models studied however the dynamic range of scales over which GS95-like turbulence is seen varies based on Alfvén Mach number

and the range of the parallel and perpendicular ambipolar diffusion scales bounded by the viscous dissipation scale and the driving scale. We found that Alfvénic turbulence does not necessarily damp at the ambipolar diffusion scale in super-Alfvénic turbulence and that the damping depends on other turbulence parameters such as the Alfvén Mach number and driving scale. We also showed that the power spectrum of the kinetic energy in the damped regime is consistent with a k^{-4} scaling, as predicted by LVC04.

B.B. acknowledges support from the NASA Einstein Fellowship. A.L. and B.B. thank the Center for Magnetic Self-Organization in Astrophysical and Laboratory Plasmas for financial support and acknowledge financial support of the INCT INEspao and the Physics Graduate Program/UFRN, at Natal, for hospitality. AL is supported by the NSF grant AST 1212096. DSB acknowledges support via NSF grants NSF-AST-1009091 , NSF-ACI-1307369 and NSF-DMS-1361197. DSB also acknowledges support via NASA grants from the Fermi program as well as NASA-NNX 12A088G. Several simulations were performed on a cluster at UND that is run by the Center for Research Computing. Computer support on NSF’s XSEDE computing resources is also acknowledged.

REFERENCES

- Ballesteros-Paredes, J., Klessen, R. S., Mac Low, M.-M., & Vazquez-Semadeni, E., 2007, *Protostars and Planets V*, 63
- Balsara, D., 1996, *ApJ*, 465, 775
- Balsara, D.S., 1998a., *ApJS*, 116, 119
- Balsara, D.S., 1998b., *ApJS*, 116, 133
- Balsara, D., 2004, *ApJS*, 151, 149
- Balsara, D.S., 2010, *J. Comp. Phys.*, 229, 1970
- Balsara, D.S., 2012, *J. Comp. Phys.*, 231, 7476
- Balsara, D. S., & Shu, C.-W., 2000, *J. Comput. Phys.*, 160, 405
- Balsara, D.S., Spicer, D., 1999a., *J. Comput. Phys.*, 148, 133
- Balsara, D.S., Spicer, D., 1999b., *J. Comput. Phys.*, 149, 270
- Balsara et al., 2008, *MNRAS*, 386, 642

- Beresnyak, A., Lazarian, A., & Cho, J., 2005, ApJ, 624, 93
- Beresnyak, A., & Lazarian, A., 2014, chapter for "Lecture Notes in Physics", in press.
- Brandenburg, A. & Zweibel, E., 1994, ApJ, 427, 91
- Brandenburg, A. & Zweibel, E., 1995, ApJ, 448, 734
- Brandenburg, A., & Lazarian, A., 2013, SSRv, 178, 163
- Burkhart et al., 2009, ApJ, 693, 250
- Burkhart et al., 2014, ApJ, accepted.
- Clark, S., E., Peek, J. E., G., Putman, M., E., 2014, ApJ, 789, 82
- Ciolek, G. & Basu, S., 2000, ApJ, 529, 952
- Cho, J. & Lazarian, A. 2002, Phys. Rev. Lett., 88, 5001
- Cho, J. & Lazarian, A., 2003, MNRAS, 345, 325
- Correia et al., 2014, ApJ, 785, 1
- Crutcher, R., Hakobian, N., Troland, T., 2009, ApJ, 692, 844
- Esquivel, A., & Lazarian, A., 2005, 631, 320
- Esquivel, A., & Lazarian, A., 2011, ApJ, 740, 117
- Goldreich, P., & Sridhar, S., 1995, ApJ, 438, 763 (GS95)
- Hezareh et al. 2014, MNRAS, 438, 663
- Jiang, G. S., & Shu, C.-W. 1996, J. Comput. Phys., 126, 202
- Klessen, R., Heitsch, F., Mac Low, M-M., 2000, ApJ, 535, 887
- Kowal, G., & Lazarian, A., 2010, ApJ, 720, 742
- Langer, W., D., 1978, ApJ, 225, 95
- Lazarian, A., & Vishniac, E., 1999, ApJ, 517, 700
- Lazarian, A., Vishniac, E., & Cho, J., 2004, ApJ, 603, 180
- Lazarian, A., 2006, ApJ, 645, 25

- Lithwick, Y, Goldreich, P., 2001, ApJ, 562, 279
- Li, P. S., McKee, C., Klein, R., 2006, ApJ, 653, 1280
- Li et al., 2008, ApJ, 684, 380
- Li, H., & Houde, M., 2008, ApJ, 677, 1151
- McKee, C., Ostriker, E., 2007, ARA&A, 45, 565
- Meyer et al. 2014, MNRAS, 439, 219
- Minter, A., Spangler, S., 1997, ApJ, 485, 182
- Oishi, J., Mac Low, M-M., 2006, ApJ, 638, 2810
- Spangler, S., 1991, ApJ, 376, 540
- Tassis, K., & Mouschovias, T., 2004, ApJ, 616, 283
- Tilley, D. A., & Balsara, D. S., 2006, ApJL, 645, 49
- Tilley, D. A., Balsara, D. S., & Howk, J. C., 2006 MNRAS, 371, 1106
- Tilley, D. A., Balsara, D. S., 2008, MNRAS, 389, 1058
- Tilley, D. A., Balsara, D. S., Meyer, C. 2012, New Astron. 17, 368
- Tilley, D. A., Balsara, D. S., 2010, MNRAS, 406, 1201
- Tilley, D. A., Balsara, D. S., 2011, MNRAS, 415, 3681
- Yan, H., Lazarian, A., 2004, ApJ, 614, 757
- Zakharov, V.E., & Sagdeev, A., 1970, Sov. Phys. Dokl., 15, 439
- Zweibel, E. G. & Josafatsson, K., 1983, ApJ, 270, 511
- Xu, S, Lazarian, A. & Yan, H. ApJ, in preparation

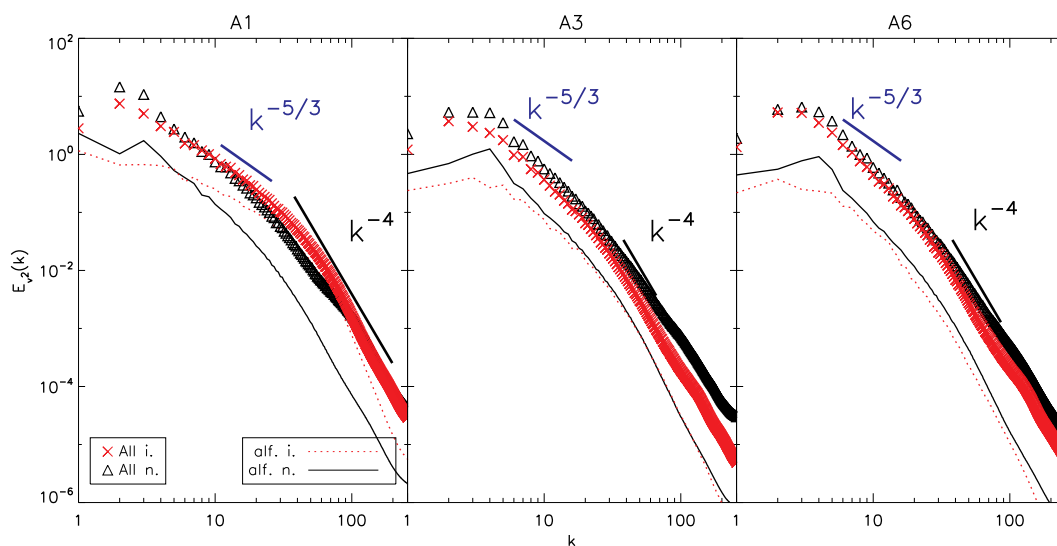


Fig. 5.— The neutral kinetic energy power spectrum (black lines) and the ion kinetic energy power spectrum (red lines) for models A1, A3 and A6. Each model has its own panel from left to right, respectively. Symbols indicate the full kinetic energy spectrum while lines indicate the energy spectrum of the Alfvén modes only. We modify the power spectrum by $k^{5/3}$, which is the predicted slope for both Alfvénic turbulence and Kolmogorov-type turbulence.